Progress In Electromagnetics Research C, Vol. 107, 113–126, 2021

Wideband Pentagonal Shape Microstrip Antenna Using a Pair of Rectangular Slots

Amit A. Deshmukh* **and Venkata A. P. Chavali**

Abstract—Designs of a polygon shape microstrip antenna for increasing number of side lengths are studied. A detailed analysis is presented for the variations observed in the first and second order mode resonance frequencies in a polygon shape patch, from triangle to square to pentagon, ending up in a circle. Among all the polygon shapes, close spacing between the first two frequencies is obtained in the pentagon shape patch. A design of a pentagon shape microstrip antenna with a pair of slots is proposed. It gives impedance bandwidth of more than 700 MHz ($> 55\%$), which is maximum amongst all the polygon shapes employing a pair of rectangular slots. The proposed design offers a peak broadside gain of 9 dBi over the bandwidth. A resonant length formulation and subsequent design methodology for the pentagon shape patch and its slot loaded variation are presented. This helps in the redesigning of a similar configuration in a given frequency range, using proximity and coaxial feeds.

1. INTRODUCTION

Microstrip antenna (MSA) in its simplest form consists of a radiating patch on one side of a microwave substrate and ground plane on the other [1–4]. The radiating patch can take any arbitrary shape, but from the fabrication and mathematical modelling point of view, regular shapes and their variations are preferred [1–3]. Initially, the MSA suffered from the disadvantage of narrow impedance bandwidth (BW). However, over the last four decades, many techniques have been reported for the BW enhancement, and among them slot cut method is widely used [4–16]. An increase in the BW of slot cut MSA is realized by employing multiple slots [17–24]. As compared with a single slot cut design, the use of multiple slots increases the BW by 10 to 15%. A detailed study to explain the functioning of wideband slot cut MSAs in terms of patch resonant modes is reported [23, 24]. It reveals that the wideband response is the result of coupling between the fundamental and modified higher order orthogonal resonant modes of the patch. In addition, slots also modify the surface current distributions at higher order patch mode to give broadside radiation pattern across the BW, with the same polarization of the radiated field. A polygon is a two-dimensional shape drawn with the help of straight lines. Triangle, square, pentagon, hexagon are the examples of polygon shapes where the number of straight lines (side lengths) is 3, 4, 5, and 6, respectively. Circular shape is also a variation of polygon in which the number of side lengths is ideally infinite or practically large.

In this paper, initially proximity fed circular MSA (CMSA) of radius 'r' = 7 cm is studied on an air substrate of thickness 'h' = 3 cm. For this patch radius, different polygon shapes namely, triangle, square, pentagon, hexagon, septagon, and octagon are realized. The frequencies corresponding to the fundamental and second order orthogonal modes for these polygons, including a circular patch, are noted. In addition, the surface current distribution at the second order orthogonal mode in each polygon is studied. Amongst all the polygons, in pentagonal shape MSA (P-MSA), lower frequency ratio between the first two frequencies with higher amount of the contribution of the horizontally directed

Received 26 October 2020, Accepted 16 November 2020, Scheduled 1 December 2020
* Corresponding author: Amit A. Deshmukh (amitdeshmukh76@gmail.com).
The authors are with the EXTC Department, SVKM's DJSCE, Mumbai, India.

surface currents at second order orthogonal mode is observed. Hence for BW enhancement, the design of P-MSA with a pair of rectangular slots is explored. The pair of slots in P-MSA tunes the interspacing between the second order TM_{21} mode frequency and fundamental TM_{11} mode, to give wider BW. The simulated and measured BW of more than 700 MHz (> 55%) is obtained. This BW is more than that obtained in other polygon shape MSAs. In addition, slot cut P-MSA design offers stable broadside gain characteristics across the BW as compared with all the other slot cut polygon MSAs. The resonant length formulation at TM_{11} and TM_{21} modes in P-MSA and slot cut P-MSA in terms of the patch and slot dimensions is presented, which gives closer prediction with the simulated frequencies. Using the proposed formulation, the procedure to redesign a wide band slot cut P-MSA in given frequency range is presented, which yields a similar wideband response using the proximity and coaxial feeds.

In the reported literature, wideband designs using slots are widely discussed. To highlight the novelty in the proposed slot cut P-MSA design, a comparison is presented in Table 2 for similar slot cut designs using other polygon shape MSAs and reported multiple slots cut design using regular shapes. The P-MSA with a pair of rectangular slots offers 10% additional BW against similar slot cut variations using CMSA and square MSA (SMSA). Against the multiple slots cut antennas, the proposed design gives equivalent or higher impedance BW and offers stable gain characteristics. In addition, it requires only single pair of slots which makes the implementation simpler. The proposed formulation is helpful in the redesigning of similar antennas around the specific resonance frequency. The MSAs discussed in this paper are initially studied using CST software [32]. For analyzing the antenna response in the present study, finite square ground plane of side length 35 cm with N-type connector feed is selected. The experimental validation for the obtained results is carried out inside the antenna lab using high frequency instruments namely, ZVH-8, FSC 6, and SMB 100A.

2. PROXIMITY FED POLYGON MSAS WITH A PAIR OF SLOTS

Proximity fed designs of polygon shape MSAs are shown in Figs. 1(a)–(h). Initially, a CMSA for radius 'r' = 7 cm on an air substrate of thickness 'h_a' = 3.0 cm and proximity strip thickness of 'h_s' = 2.8 cm is studied. In simulations, the circular patch is drawn using 24 side lengths. For the given CMSA dimensions, and TM_{11} mode frequency is found to be 940 MHz. The simulations were also carried out using more than 24 side lengths, which show marginal variation in the patch frequency. Hence, 24 side lengths are considered in CMSA. For the same patch radius, various polygon MSAs, namely,

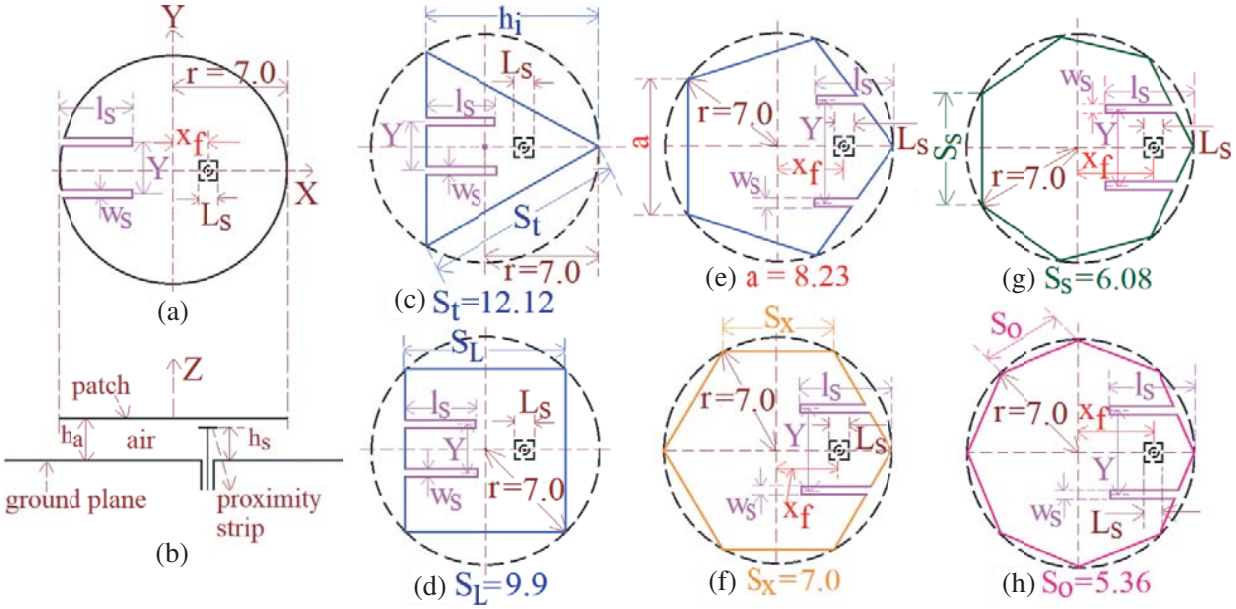

Figure 1. Proximity fed Polygon MSAs. (a) Top and (b) side views of CMSA, (c) ETMSA, (d) SMSA, (e) P-MSA, (f) Hexagonal MSA, (g) Septagon MSA and (h) Octagon MSA (all units in cm).

equilateral triangular MSA (ETMSA), SMSA, P-MSA, hexagonal MSA, septagon MSA, and octagon MSA are realized as shown in Fig. 1. In ETMSA, three vertex points are separated by 120, and '$2h_i/3$' equals the patch radius 'r'. Various patch dimensions in all the polygon MSAs are shown in Fig. 1. For the proximity feed location shown, all the variations were simulated over a wide frequency range. The frequencies corresponding to the fundamental and second order modes were noted. Against the increasing number of side lengths in polygon MSAs, the dual frequencies and their ratio plots are given in Fig. 2(a). Also the surface current distributions at second order mode in various polygon MSAs are studied, as shown in Figs. 2(b)–(g).

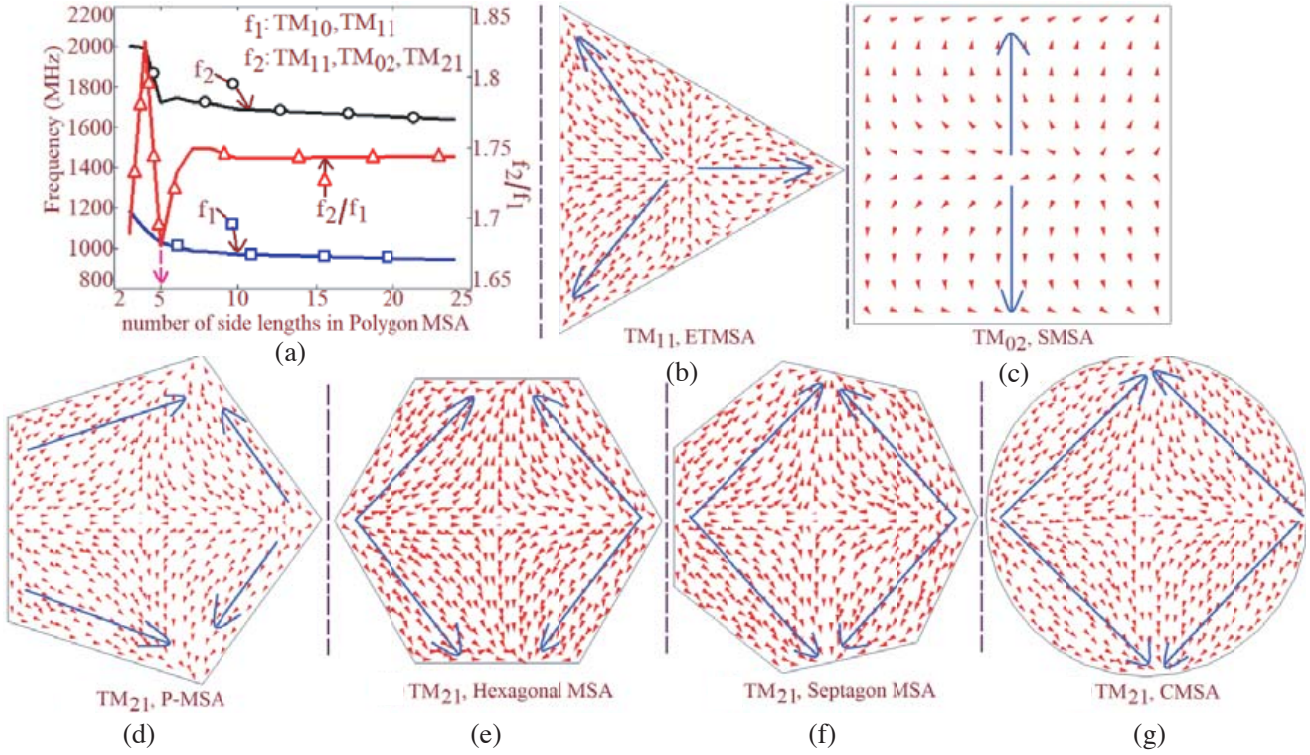

Figure 2. (a) Dual frequencies and their ratio plots against increasing number of side lengths and (b)–(g) surface current distribution at second order mode in various Proximity fed Polygon MSAs.

The fundamental mode in ETMSA and SMSA is TM_{10} whereas in other polygon MSAs, it is TM_{11} [1–4]. The second order mode in ETMSA is TM_{11} whereas in SMSA it is TM_{02} [1–4]. In rest of the polygon MSAs, second order mode is referred to as TM_{21}, as the surface currents at them exhibit similar variations to that observed in TM_{21} resonant mode in CMSA [1–4]. Due to the smaller patch area, TM_{10} and TM_{11} mode frequencies are higher in ETMSA. With the increase in number of side lengths in polygon MSA, frequencies of the first and second order modes decrease. This reduction in the frequencies is attributed to the increase in patch area with number of side lengths. As observed from the current distribution of TM_{21} mode in P-MSA, due to the pentagonal geometry, vector current lengths are larger in dimension than the TM_{21} mode current vectors in hexagonal MSA. Due to this TM_{21} mode frequency is lowered in P-MSA. This leads to the lowest frequency ratio (f_2/f_1) between the first two modes in P-MSA. Also as seen from the surface current plots at second order mode, vertical components of the surface currents in P-MSA are smaller in contribution than the other polygon shape MSAs. These smaller vertical current components will lead to the lower cross-polar radiation in its broadband configuration when the TM_{21} mode frequency in P-MSA is tuned with respect to the TM_{11} mode. Due to these two features of the pentagonal shape geometry, the design of the P-MSA loaded with a pair of slots is investigated for the BW enhancement as shown in Fig. 1(e). The pair of slots is cut on that patch edge in P-MSA, where surface currents are more vertically aligned as shown in Figs. 2(d)

and 1(e). Further to tune the TM_{21} and TM_{11} mode frequencies, parametric study is carried out for the increment in slot length 'l_s', and the simulated resonance curve plots for them are shown in Fig. 3(a). With an increase in 'l_s', frequency of the TM_{21} mode decreases as the surface currents are orthogonal to the slot length. The TM_{11} mode frequency remains unchanged. Thus, slot yields optimum spacing between the TM_{21} and TM_{11} mode frequencies to realize wideband response as shown in Fig. 3(b). For 'l_s' = 3.0, 'Y' = 6, 'w_s' = 0.6, and 'x_f' = 3.2 cm, the simulated BW is 737 MHz (57.69%). Simulated BWs realized in other polygon shape MSAs with a pair of slots are ETMSA (534 MHz, 39.82%), SMSA (572 MHz, 44%), hexagonal MSA (663 MHz, 52.9%), septagon MSA (628 MHz, 51.6%), octagon MSA (545 MHz, 46.5%), and CMSA (492 MHz, 43.4%). Thus, BW obtained in slot cut P-MSA is much higher than that obtained in other polygon shape MSAs. Further, slot cut P-MSA was fabricated using a copper plate and was suspended in air using foam spacers support, placed towards the antenna corners. The BW obtained using the measurement is 725 MHz (57.75%) as shown in Fig. 3(b). The fabricated slot cut P-MSA design is shown in Figs. 3(c), (d).

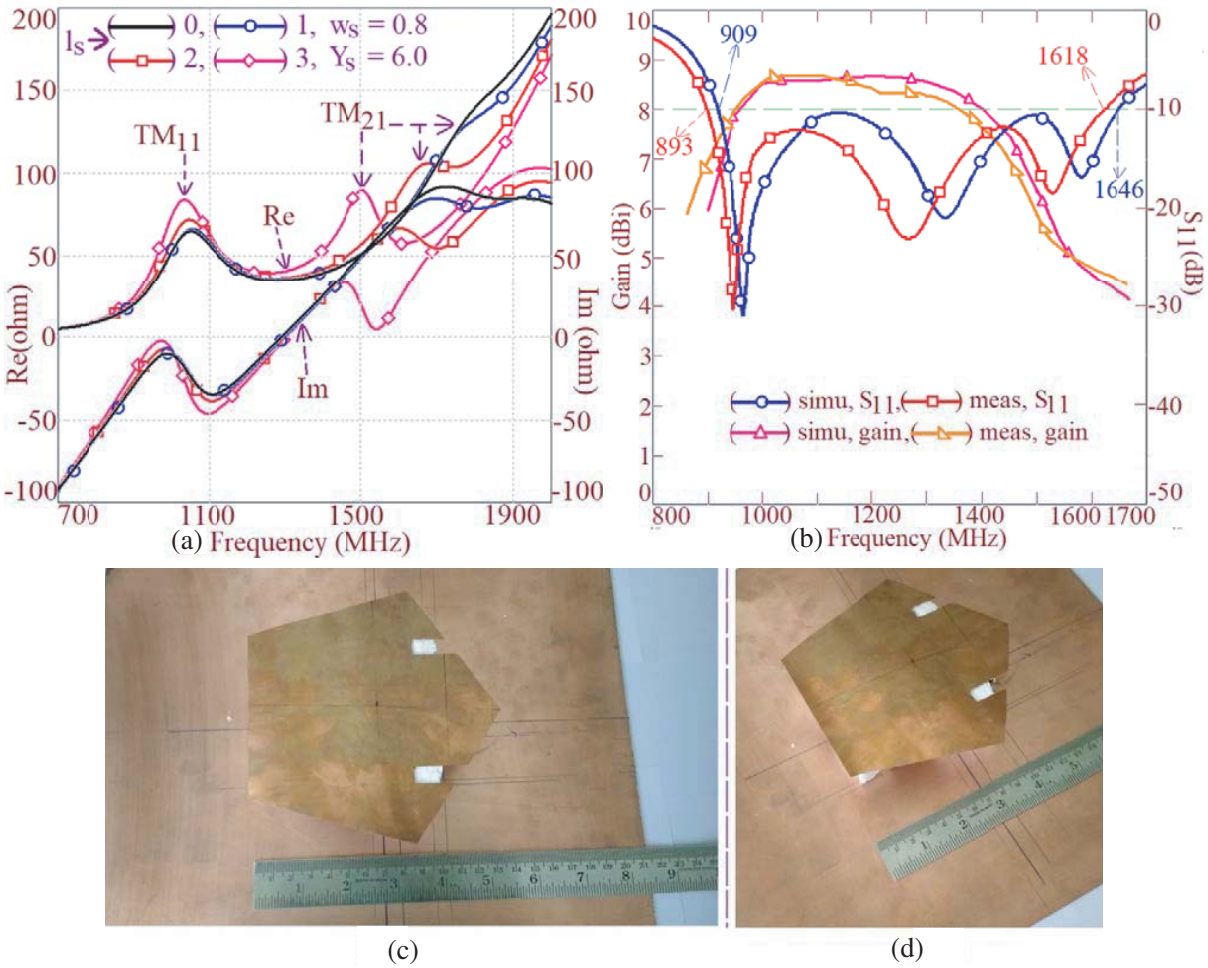

Figure 3. (a) Resonance curve plots for increase in 'l_s', (b) return loss (S_{11}) and gain plots for the optimum design and (c), (d) fabricated prototype of the P-MSA with a pair of slots.

The peak broadside antenna gain as shown in Fig. 3(b) is close to 9 dBi. The slot cut P-MSA offers stable gain characteristics over most of the VSWR BW. To compare the gain performances, simulated broadside gain plots in all the slot cut polygon MSA variations are shown in Fig. 4(a). In slot cut CMSA and SMSA, broadside gain varies over the impedance BW. In comparison, the proposed design of a P-MSA with a pair of slots offers stable gain characteristics against them as well as other slot cut

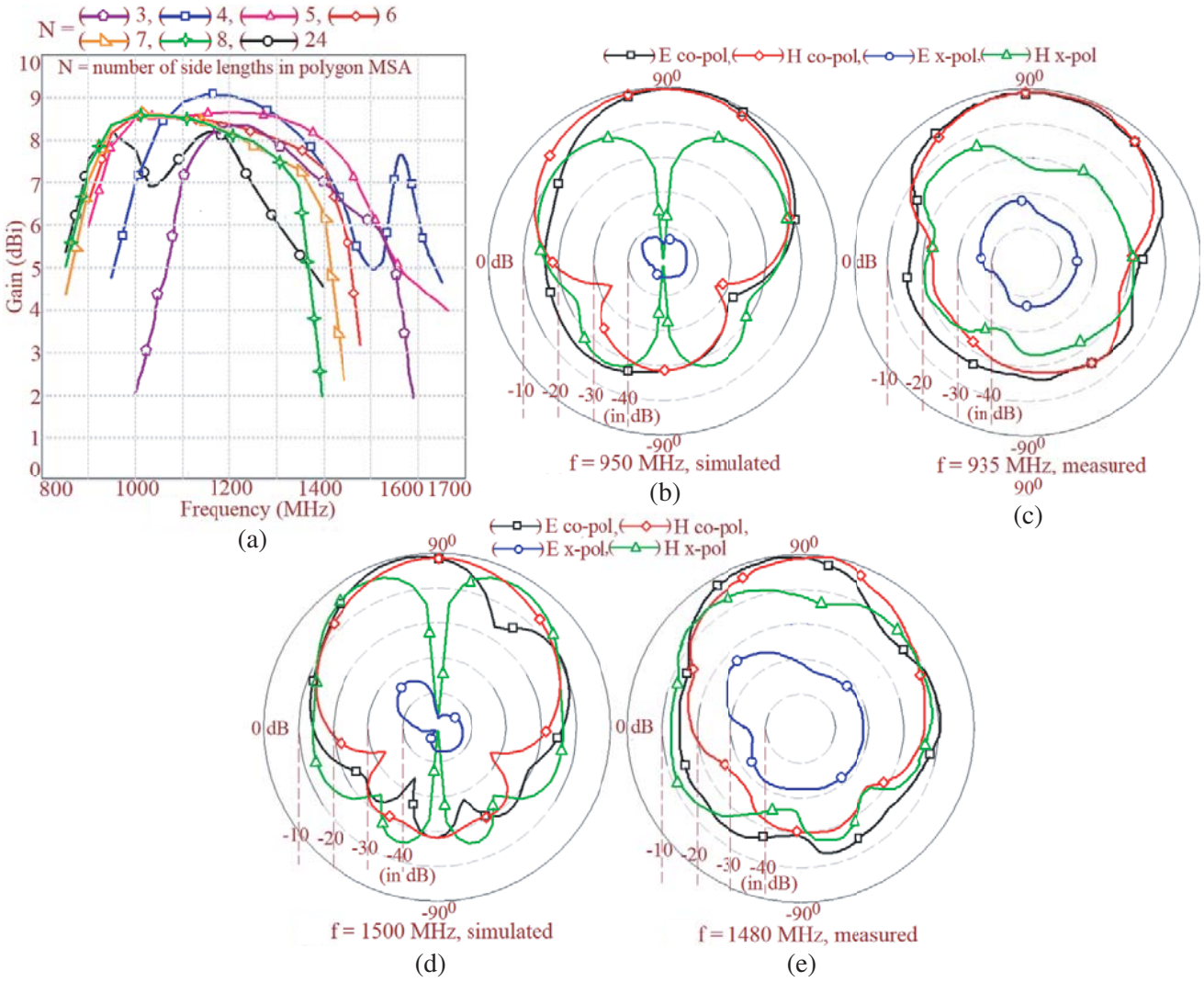

Figure 4. (a) Gain variation over the BW in various polygon MSA variations and (b)–(e) radiation pattern nearer to the band start and stop frequencies in a P-MSA with a pair of slots.

polygon MSA variations. The radiation pattern close to the band start and stop frequencies of the BW is shown in Figs. 4(b)–(e). At the two frequencies shown and as observed across the entire BW, radiation pattern remains in the broadside direction with E- and H-planes aligned along $\Phi = 0°$ and 90°, respectively. Over the complete BW, cross polar radiation remains below 10 dB as compared with the co-polar levels in the broadside direction. In the next section, resonant length formulations at the two modes in P-MSA are presented.

3. RESONANT LENGTH FORMULATION FOR THE P-MSA WITH A PAIR OF SLOTS

The surface current distributions at TM_{11} and TM_{21} resonant modes in P-MSA are similar in variation to the current variations present in CMSA. Hence, the resonance frequency equation of CMSA can be used for P-MSA. However, there exists the difference in the patch areas of P-MSA and CMSA, due to which fundamental mode frequency of P-MSA is greater than the fundamental mode frequency in CMSA. Therefore, initially the equivalence is established in between the areas of P-MSA and CMSA to express the side length of P-MSA in terms of the radius of equivalent circular patch. For a regular

P-MSA with side length 'a' and radius 'r', the patch area is calculated by using Equation (1). This area is equated to the area of the circular patch of radius 'r_c', which gives the relation between the P-MSA side length and equivalent radius 'r_c' as given in Equation (2). Using this, resonance frequency equation for CMSA is modified to realize the resonance frequency equation for P-MSA as given in Equation (3).

$$A_p = a^2\sqrt{5\left(5+2\sqrt{5}\right)}\Big/4 = 1.72a^2 \tag{1}$$

$$r_c = a\sqrt{1.72/\pi} \tag{2}$$

$$f_{mn} = K_{mn}c/4.649a\sqrt{\varepsilon_{re}} \tag{3}$$

where 'c' is the velocity of light in free space, and 'K_{mn}' are the Bessel function coefficients.

Further, the effects of the pair of rectangular slots on TM_{11} and TM_{21} mode frequencies in the pentagon patch are formulated. Since the surface currents at two modes are similar in variation to that observed in CMSA, patch radius is modified first for formulating the slot effect. At TM_{11} mode, although the surface currents are parallel to the slot length, finite slot width perturbs the current path length as shown in Fig. 5(a). By accounting for this perturbation and the edge extension length due to the fringing fields, an equation for the effective patch radius is formulated as given in Equation (4). Later, the effective side length is calculated by using its geometric relation with the patch radius as given in Equation (5). The calculated TM_{11} mode resonance frequency and % error between the simulated and calculated values are obtained by using Equations (6) and (7), respectively. Against the slot length variation, two frequencies and % error are shown in Fig. 5(c). For the complete slot length range, a close prediction between the two frequencies with % error less than 3% is obtained.

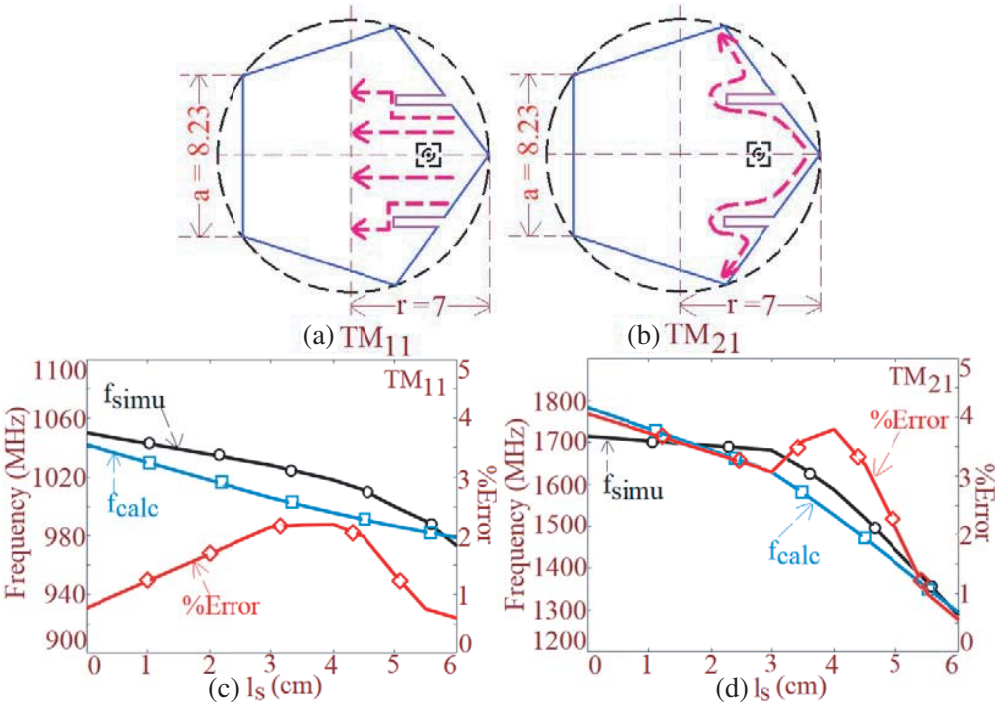

Figure 5. Schematic of the resonant length formulation at (a) TM_{11} and (b) TM_{21} modes and frequency and % error plots at (c) TM_{11} and (d) TM_{21} modes for proximity fed P-MSA with a pair of slots.

At TM_{11} mode,

$$r_{e11} = r + 0.9h + (w_s \sin(\pi l_s/3r)) \tag{4}$$

$$a_{e11} = 2r_{e11}\sin(36\pi/180) \tag{5}$$

$$f_{11} = 1.84118c/4.649a_{e11}\sqrt{\varepsilon_{re}} \tag{6}$$

$$\%Error = |f_{calc} - f_{simu}/f_{simu}| \times 100 \tag{7}$$

The variations in surface currents at TM_{21} mode against the slot length increment were further studied. The current vectors were found circulating around the slot length as shown in Fig. 5(b). The effective patch radius at TM_{21} mode is obtained by adding this effect as given in Equation (8). Further, the effective side length and the frequency are calculated by using Equations (9) and (10), respectively. The simulated and calculated TM_{21} mode frequencies and the % error between them are plotted in Fig. 5(d). For all the values of the slot lengths, a close agreement between the two frequencies is obtained. Further using the proposed formulation, the procedure to design the P-MSA with a pair of slots using the proximity and coaxial feed is put forward.

At TM_{21} mode,

$$r_{e21} = r + 0.8h + 2l_s\,(l_s/2r)\sin\left(2Y\pi/3a\right) \tag{8}$$

$$a_{e21} = 2r_{e21}\sin\left(36\pi/180\right) \tag{9}$$

$$f_{21} = 3.05424c/4.649a_{e21}\sqrt{\varepsilon_{re}} \tag{10}$$

4. DESIGN PROCEDURE FOR P-MSA WITH A PAIR OF SLOTS

As seen from the optimum results in the P-MSA with a pair of slots, band start frequency is closer to the TM_{11} mode frequency of the patch without the slot. Thus, to design broadband antenna, initially TM_{11} mode frequency is selected. At this frequency, air substrate thickness for the patch is selected to be $0.1\lambda_0$. For this frequency, effective patch side length (a_e) in P-MSA is calculated by using Equation (11). The patch radius for this side length is calculated by using Equation (12). For this radius, actual P-MSA side length 'a' is calculated by using Equation (5). The position of the pair of slots from the patch center ($Y/2$) and slot width (w_s) are taken equal to $0.105\lambda_0$ and $0.028\lambda_0$, respectively. The proximity feeding strip parameters are selected as $h_s = 0.091\lambda_0$, $L_s = 0.056\lambda_0$, and $x_f = 0.1085\lambda_0$. These parameters are selected based upon their optimum design values as present in the above proximity feed design.

$$a_e = 1.84118c/4.649f_{11}\sqrt{\varepsilon_{re}} \tag{11}$$

$$r = (a_e/2\sin\left(36\pi/180\right)) - 0.9h \tag{12}$$

Further by using Equations (4)–(10), calculated TM_{11} and TM_{21} mode frequencies and their ratio plots against increasing slot length 'l_s' are generated. In the above optimum design, the frequency ratio between TM_{21} and TM_{11} modes for the maximum BW is around 1.45. Therefore from the generated frequency plots, slot length is noted that ratio '$f_{TM_{21}}/f_{TM_{11}}$' is around 1.45. Using this procedure, the P-MSA with a pair of slots is designed for TM_{11} = 800, 1500, and 2500 MHz. The dual frequencies and their ratio plots at the three frequencies are shown in Figs. 6(a)–(c). The slot length is noted, which

Table 1. Various antenna parameters for slot cut P-MSA.

Parameter (cm)	800 MHz (air)	1500 MHz (air)	2500 MHz (air)	3000 MHz (FR4)	4250 MHz (Arlon)
r	93	4.9	2.95	2.2	1.4
a	10.93	5.76	3.47	2.6	1.65
h_a	3.75	2.0	1.2	0.48	0.32
h_s	3.4	1.8	1.1	—	—
L_s	1.9	1.1	0.65	—	—
x_f	4.1	2.0	1.3	1.1	0.55
l_s	6.3	3.4	2.1	1.6	1.0
Y	7.8	4.2	2.5	0.8	0.55
w_s	1.0	0.6	0.3	0.1	0.1
Simu BW (MHz, %)	577, 58.67	1051, 57.6	1718, 57.23	622, 18.4	1070, 21.96

gives frequency ratio of 1.45. Antennas at the three TM_{11} mode frequencies are designed using the above procedure. Various antenna parameters at these frequencies are given in Table 1. To realize the optimum response, marginal parametric optimization is needed further as using the above procedure, and non-integer values are obtained for some of the antenna parameters which are rounded off to the nearest integer or the practically realizable value. In each variation, wideband response is obtained as

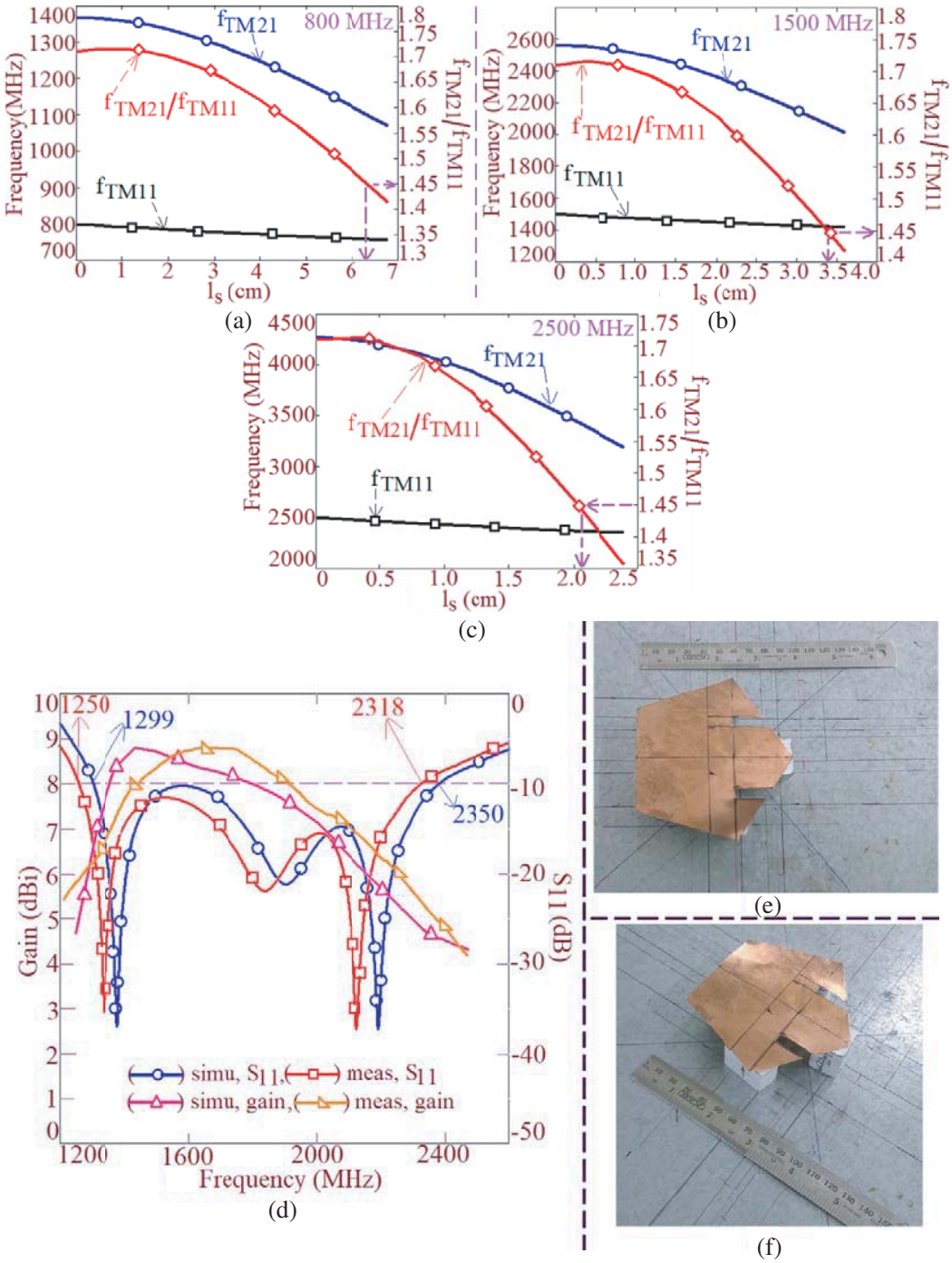

Figure 6. Dual frequencies and their ratio plots in slot cut P-MSA for TM_{11} = (a) 800, (b) 1500 and (c) 2500 MHz, (d) return loss and gain plots, and (e), (f) fabricated prototype for proximity fed P-MSA with a pair of slots at 1500 MHz.

given in Table 1. The measurements were carried out, and the results for the design at 1500 MHz are shown in Figs. 6(d)–(f). Here the measured BW is 1068 MHz (59.86%) which is in close agreement with the simulated value as mentioned in Table 1. The peak antenna gain is close to 9 dBi. The antenna shows a gain above 6 dBi over most of the BW. At other frequencies, close matching of the measured BW against the simulated BW is also obtained. Next using the proposed formulations, the design of slot cut P-MSA is presented using the coaxial feed.

As per the reported literature, coaxially fed slot cut MSAs are optimized on substrate thickness in the range of $0.06 - 0.08\lambda_g$. As for the thickness greater than $0.08\lambda_g$, larger probe inductance limits the antenna BW, whereas for the thickness lower than $0.06\lambda_g$, larger capacitive impedance formed due to the pair of slots limits the antenna BW [4, 5, 24]. Hence here the design is presented for the total substrate thickness of $0.06\lambda_g$ using air suspended microwave substrates. At $f_{TM11} = 3000$ MHz, the design is presented on a suspended FR4 substrate ($h_{sub} = 0.159$ cm, $\varepsilon_r = 4.3$), and for $f_{TM11} = 4250$ MHz, the design is presented using a suspended Arlon substrate ($h_{sub} = 0.159$ cm, $\varepsilon_r = 4.5$). The air suspended substrates are chosen to achieve higher radiation efficiency and gain. For the given TM_{11} mode frequency, P-MSA radius on air suspended substrate is calculated by using Equations (11) and (12). The effective

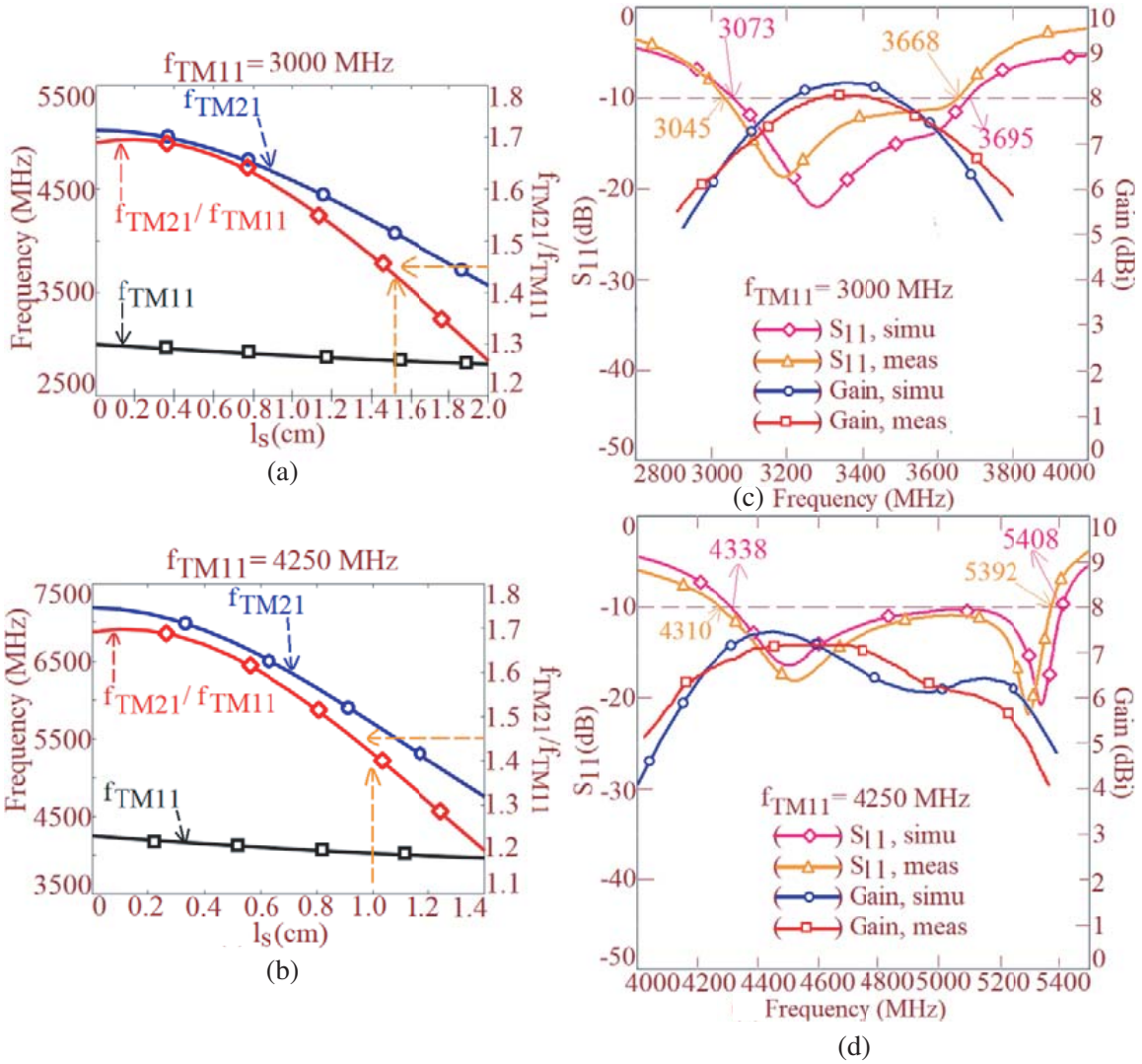

Figure 7. Dual frequencies and ratio plots for slot cut P-MSA at (a) 3000 and (b) 4250 MHz, and return loss and gain plots at (c) 3000 and (d) 4250 MHz.

dielectric constant (ε_{re}) is calculated by using Equation (13).

$$\varepsilon_{re} = 1.189\varepsilon_r\,(h + h_a)/\varepsilon_r h_a + h \tag{13}$$

'h' in Equation (12) equals $0.06\lambda_g$ that equals the substrate thickness (h_{sub}) plus the air gap. The practically realizable value of the air gap is chosen that gives the total substrate thickness of $0.06\lambda_g$. 'λ_g' is the wavelength in the suspended dielectric. The position of the pair of slots from the patch center and the slot width are taken equal to $0.105\lambda_g$ and $0.028\lambda_g$, respectively. The coaxial feed is placed at a distance of 'x_f' $= 0.1085\lambda_g$ from the patch center. Further, the dual frequencies and their ratio plots are generated for the coaxial fed P-MSA against the increase in the slot length. At the two TM_{11} mode frequencies, they are shown in Figs. 7(a), (b).

From the plots, slot length is selected which gives frequency ratio of around 1.45. Slot cut P-MSAs using coaxial feed are designed using this procedure, and the antenna parameters for them are given in Table 1. The value of 'h_a' as mentioned in Table 1 is the total substrate thickness. For the design at 3000 MHz, the air gap of 0.32 cm is present whereas at 4250 MHz, air gap is 0.16 cm. The results for the two designs are shown in Figs. 7(c), (d). At 3000 MHz, simulated BW is 622 MHz (18.4%) whereas at 4250 MHz, simulated BW is 1070 MHz (21.96%). A smaller BW than the air suspended design is attributed to the lower substrate thickness as well as the absence of proximity feed. The band start frequency in the two coaxial feed designs is close to the TM_{11} mode frequency of P-MSA. Further, the measurements were carried out to validate the simulations, and their results are shown in Figs. 7(c), (d). At 3000 MHz, the measured BW is 623 MHz (18.56%) whereas at 4250 MHz, the measured BW is 1082 MHz (22.3%). The gain over most of the BW is above 6 dBi in both the designs. A broadside radiation pattern across the BW is observed. The fabricated antenna prototypes at two frequencies are shown in Figs. 8(a) and 8(b), respectively. Thus, the proposed design methodology is useful in realizing the wideband response close to the given TM_{11} mode frequency of the P-MSA, using the proximity or coaxial feed.

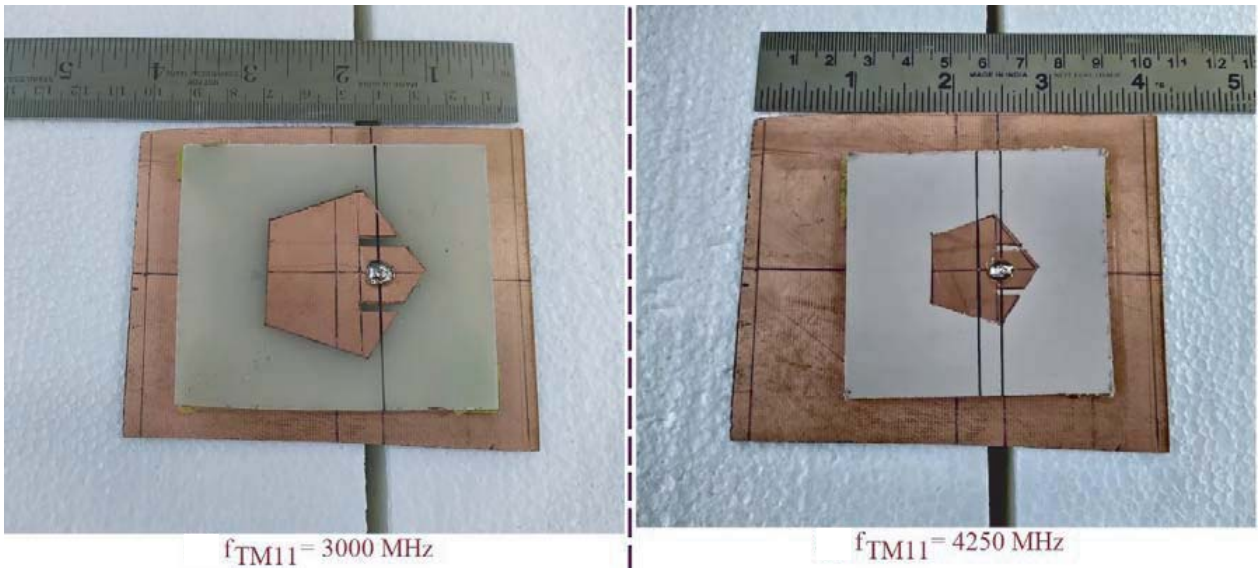

Figure 8. Fabricated antenna prototypes at (a) 3000 and (b) 4250 MHz for coaxially fed MSAs.

To highlight the novelty in the proposed slot cut P-MSA, a detailed comparison of the other polygon shape MSAs using a pair of slots and the reported slot cut wideband variations is shown in Table 2. The patch area and substrate thickness as mentioned in Table 2 are normalized with respect to the wavelength (λ_c) at the center frequency of the realized impedance BW. As compared with the other slot cut polygon shape MSAs, the proposed P-MSA offers larger BW with better gain characteristics. Although the proposed design requires thicker substrates than the designs reported in [5–7], it offers higher BW with

comparable or lower patch size. The design reported in [10] requires smaller patch size and substrate thickness but shows gain variation over the BW. In comparison, the proposed design offers higher BW and stable gain response. Compared with the MSA reported in [13], which uses corrugation along the patch width, the proposed design is simpler to fabricate. The wideband configurations in [14, 15] require differential feeding and larger patch size for effective tuning of TM_{10} and TM_{30} mode frequencies. In comparison, the proposed design employs simpler proximity feed and offers wider BW with smaller patch size. Although the antenna reported in [16] offers wider BW, it suffers from the disadvantage of gain variation, because of the orthogonal currents present at the modified higher order modes. The design reported in [18] offers higher BW on lower substrate thickness. However, it requires differential feeding, and the radiation pattern does not remain in the broadside direction over the entire BW. Compared with the multiple slots cut design reported in [19–24], the proposed antenna offers comparable values of the BW but requires only single pair of rectangular slots. The designs of slot cut isosceles MSAs yield

Table 2. Comparison of the P-MSA with a pair of slots against polygon shape MSAs and reported slot cut designs.

MSA reported in	Meas BW (MHz, %)	Patch area (A_p/λ_c)	Peak Gain (dBi)	Substrate thickness (h/λ_c)
Fig. 1(e)	**725, 57.75**	**4.874**	**8.7**	**0.125**
Fig. 1(a)	480, 43.16	5.71	8.2	0.112
Fig. 1(d)	564, 43.92	4.194	9.1	0.128
Fig. 1(f)	653, 52.77	5.249	8.5	0.124
Ref. [5]	470, 44.9	9.54	10	0.08
Ref. [6]	408, 24.82	3.74	7.2	0.076
Ref. [7]	172, 19.9	5.616	8.5	0.062
Ref. [10]	700, 31	1.672	8.5	0.07
Ref. [11]	874, 23	0.95	—	0.2
Ref. [13]	1150, 21	1.378	10	0.036
Ref. [14]	380, 14.8	6.848	9.9	0.06
Ref. [15]	260, 13	7.301	7	0.037
Ref. [16]	3550, 62.3	1.316	7.85	0.133
Ref. [17]	700, 44	5.975	9.9	0.09
Ref. [18]	2040, 67.5	2.294	9.5	0.023
Ref. [19]	580, 27.62	2.93	9.41	0.101
Ref. [20]	3000, 53.6	2.1	10.2	0.124
Ref. [23]	590, 53.9	7.11	8.0	0.104
Ref. [24]	521, 47.4	11.4	9.4	0.109
Ref. [25], 100 ITMSA with slots	882, 62.11	6.286	8.5	0.142
Ref. [25], 90 ITMSA with U-slot	810, 63.2	5.725	9.0	0.128
Ref. [26]	415, 42	8.233	9.0	0.1
Ref. [27]	350, 6.8	0.83	7.0	0.043
Ref. [28] half U-slots + rectangular slot	1345 61	4.02	8.1	0.134

higher BW than proposed P-MSA design [25]. However, they require larger patch size and show larger variation in the broadside gain over the BW. The designs using multiple patches and slots reported in [26] offer larger patch size with smaller BW than the proposed configuration. The broadband MSA reported in [27] is optimized on a thinner substrate and thus has smaller patch size. Due to this it has smaller BW and gain. Although the design reported in [28] yields BW of above 60%, it uses two half U-slots and rectangular slots, which makes their design complex. Against that, proposed design uses single pair of slots and offers comparable values of the BW and gain. Over the entire VSWR BW, cross polar levels in the proposed design are in the range of 10 to 15 dB below the co-polar levels in the broadside direction. Therefore, similar to the design in [28], higher cross polar levels will lead to the proposed antenna being suitable in the mobile communication application. The dual wideband design using stacked variation of U-slot cut RMSA and E-shape MSA is reported in [29]. The proposed MSA offers higher BW than the BW obtained in two bands in the stacked variation.

In all the above reported papers, the design formulation to realize a similar antenna in a specific frequency band is not discussed. The proposed work presents resonant length formulation and subsequent design methodology using proximity and coaxial feeds. Recently, characteristics mode theory has been applied to analyze the wideband and circular polarized response in MSAs [11, 30, 31]. The present paper applies resonant mode based approach which exists in the given patch . The two approaches (i.e., resonant mode and characteristics mode) are similar, but in our opinion, the resonant mode based approach is simpler and provides similar insight into the antenna functioning to that would be given by characteristics mode theory. Further, characteristics mode theory approach does not give direct values of the antenna parameters for the optimum design, which are obtained here using resonant mode based approach based on the resonant length formulations and subsequent design methodology.

To summarize, the proposed work discusses the wide band variations of polygon shape MSA for different numbers of side lengths. It is found that amongst all the polygon shapes, pentagonal shape design offers better performance in terms of the BW and gain. Such a kind of detailed study for exploring the various shapes of polygon has not been discussed in the reported literature. In addition, the proposed slot cut pentagonal shape patch offers better results in terms of BW and gain than the reported variations for different numbers of slots and the feeding techniques. Thus, the simpler design of slot cut P-MSA offering wider BW supported with detailed design methodology is the new contributions in the proposed work. Polygon shapes beyond octagon were not discussed as they have nearly the same frequency values at the first two resonant modes as compared with the circular patch. The main focus of the proposed study was to explore various polygon shapes for the wideband designs. With the realized antenna characteristics like BW, gain, and cross polar radiation, the proposed design can find applications in the mobile communication systems as the base station antennas.

5. CONCLUSIONS

Designs of polygon shape MSAs for increasing number of side lengths are studied. In terms of the separation between the first two frequencies and current distribution at second order mode, pentagon MSA offers better performance. Further, variation of P-MSA with a pair of rectangular slots is proposed which yields BW of larger than 700 MHz ($> 55\%$). This BW is maximum among all the polygon MSA variations. In addition, it offers stable gain performance against the other polygon shape MSA variations. The BW offered by the proposed design is larger tan or comparable to many of the reported multiple slots cut variations, but by using only single pair of slots. The proposed configuration uses simple proximity or coaxial feeding technique, and thus it is easy to fabricate as compared with some of the reported slot cut variations.

REFERENCES

1. Garg, R., et al., *Microstrip Antenna Design Handbook*, Artech House, USA, 2001.
2. Kumar, G. and K. P. Ray, *Broadband Microstrip Antennas*, 1st Edition, USA, Artech House, 2003.
3. Bahl, I. J. and P. Bhartia, *Microstrip Antennas*, Artech House, USA, 1980.
4. Wong, K. L., *Compact and Broadband Microstrip Antennas*, 1st Edition, USA, John Wiley & Sons, New York, 2002.

5. Huynh, T. and K. F. Lee, "Single-layer single-patch wideband microstrip antenna," *Electronics Letters*, Vol. 31, No. 16, 1310–1312, August 1995.
6. Wong, K. L. and W. H. Hsu, "A broadband rectangular patch antenna with pair of wide slits," *IEEE Transactions on Antennas & Propagation*, Vol. 49, No. 9, 1345–1347, September 2001.
7. Deshmukh, A. A. and G. Kumar, "Compact broadband E-shaped microstrip antennas," *Electronics Letters*, Vol. 41, No. 18, 989–990, September 2005.
8. Bhardwaj, S. and Y. R. Samii, "A comparative study of C-shaped, E-shaped, and U-slotted patch antennas," *Microwave and Optical Technology Letters*, Vol. 54, No. 7, 1746–1756, July 2012.
9. Lee, K. F., S. L. S. Yang, A. A. Kishk, and K. M. Luk, "The versatile U-slot patch antenna," *IEEE Antennas and Propagation Magazine*, Vol. 52, No. 1, 71–88, May 2010.
10. Khodaei, G. F., J. Nourinia, and C. Ghobadi, "A practical miniaturized U-slot patch antenna with enhanced bandwidth," *Progress In Electromagnetic Research B*, Vol. 3, 47–62, 2008.
11. Khan, M. and D. Chatterjee, "Characteristic mode analysis of a class of empirical design techniques for probe-fed, U-slot microstrip patch antennas," *IEEE Transactions on Antennas & Propagation*, Vol. 64, No. 7, 2758–2770, April 2016.
12. Costanzo, S. and A. Costanzo, "Compact MUSA: Modified U-slot patch antenna with reduced cross-polarization," *IEEE Antennas and Propagation Magazine*, Vol. 57, No. 3, 71–80, July 2015.
13. Ge, Y., K. P. Esselle, and T. S. Bird, "A compact E-shaped patch antenna with corrugated wings," *IEEE Transactions on Antennas & Propagation*, Vol. 54, No. 8, 2411–2413, August 2006.
14. Liu, N. W., et al., "A low-profile wideband aperture-fed microstrip antenna with improved radiation patterns," *IEEE Transactions on Antennas & Propagation*, Vol. 67, No. 1, 562–567, October 2019.
15. Liu, N. W., et al., "A differential-fed microstrip patch antenna with bandwidth enhancement under operation of TM_{10} and TM_{30} modes," *IEEE Transactions on Antennas & Propagation*, Vol. 65, No. 4, 1607–1614, February 2017.
16. Ang, I. and B. L. Ooi, "Broadband semi-circle-fed microstrip patch antennas," *IET Microwave Antenna & Propagation*, Vol. 1, No. 3, 770–775, June 2007.
17. Guo, Y. X., et al., "Double U-slot rectangular patch antenna," *Electronics Letters*, Vol. 34, No. 19, 1805–1806, September 1998.
18. Radavaram, S. and M. Pour, "Wideband radiation reconfigurable microstrip patch antenna loaded with two inverted U-slots," *IEEE Transactions on Antennas & Propagation*, Vol. 67, No. 3, 1501–1508, December 2018.
19. Islam, M. T., M. N. Shakib, and N. Misran, "Multi-slotted microstrip patch antenna for wireless communication," *Progress In Electromagnetic Research Letters*, Vol. 10, 11–18, 2009.
20. Sharma, S. K. and L. Shafai, "Performance of a novel Ψ-shaped microstrip patch antenna with wide bandwidth," *IEEE Antennas Wireless Propagation Letters*, Vol. 8, 468–471, April 2009.
21. Ansari, J. A., et al., "Broadband rectangular microstrip antenna loaded with double U-shaped slot," *International Journal of Microwave and Optical Technology Letters*, Vol. 6, No. 4, 185–190, July 2011.
22. Neves, E. S. et al., "Single layer rectangular patch antenna with two pair of parallel slits," *Microwave and Optical Technology Letters*, Vol. 37, No. 5, 355–359, June 2003.
23. Deshmukh, A. A., D. Singh, and K. P. Ray, "Modified designs of broadband E-shape microstrip antennas," *Sadhana-Academy Proceedings in Engineering Science*, Vol. 3, No. 3, 44–64, Springer Publication, March 2019.
24. Deshmukh, A. A. and K. P. Ray, "Analysis of broadband Ψ-shaped microstrip antennas," *IEEE Antennas and Propagation Magazine*, Vol. 55, No. 2, 107–123, June 2013.
25. Deshmukh, A. A., S. Nagarbowdi, and K. P. Ray, "Broadband variations of Isosceles Triangular Microstrip Antennas (ITMSAs)," *IEEE Antennas and Propagation Magazine*, Vol. 60, No. 2, 34–47, April 2018.
26. Deshmukh, A. A. and K. P. Ray, "Broadband proximity fed modified rectangular microstrip antennas," *IEEE Magazine on Antennas and Propagation*, Vol. 53, No. 5, 41–56, October 2011.

27. Yoo, J.-U. and H.-W. Son, "A simple compact wideband microstrip antenna consisting of three staggered patches," *IEEE Antennas and Wireless Propagation Letters*, Early Access, September 2020.
28. Venkata, A., P. Chavali, and A. A. Deshmukh, "Half U-slot and rectangular slot loaded nearly square microstrip antennas for wideband response," *Progress In Electromagnetic Research C*, Vol. 104, 129–141, 2020,
29. Liu, S., W. Wu, and D.-G. Fang, "Single-feed dual-layer dual-band E-shaped and U-slot patch antenna for wireless communication application," *IEEE Antennas and Wireless Propagation Letters*, Vol. 15, 468–471, July 2015.
30. Perli, B. R. and A. M. Rao, "Characteristics mode analysis of wideband microstrip antenna," *Progress In Electromagnetic Research C*, Vol. 97, 201–212, 2019.
31. Chen, Y. and C.-F. Wang, "Characteristic-mode-based improvement of circularly polarized U-slot and E-shaped patch antennas," *IEEE Antennas and Wireless Propagation Letters*, Vol. 11, 1474–1477, 2012.
32. CST Microwave studio, Version 2019.